Thermodynamics of cumulus clouds

Stephan R. DE ROODE

Koninklijk Nederlands Meteorologisch Instituut
roode@knmi.nl

(Received 9 February 2007; received in revised form 6 June 2007; accepted 7 June 2007)

ABSTRACT:
Mixing diagrams are investigated to explore whether mixing of undiluted (adiabatic) cumulus cloud air with clear air from its environment can lead to buoyancy reversal, i.e. mixed parcels that are saturated and negatively buoyant with respect to the dry environment. It is demonstrated that buoyancy reversal will always occur at any mixing height. It is also shown that the virtual potential temperature difference between a mixed parcel and the environment is most negative at the top of the cloud. The role of the mean state structure on the buoyancy of mixed parcels is discussed. The analytic expression describing the form of the mixing diagram is shown to be identical to the cloud-top entrainment instability criterion originally derived for a stratocumulus cloud layer capped by an inversion.
Key words: cumulus clouds, mixing diagrams, lateral mixing, buoyancy reversal.

Termodinámica de Nubes Cúmulo

RESUMEN:
Se investigan diagramas de mezcla para explorar si la mezcla de aire no diluida de las nubes cúmulo (adiabática) con aire no nuboso del entorno puede llevar a una inversión de la flotabilidad, es decir masas de aire mezcladas que son saturadas y con flotabilidad negativa con respecto al aire circundante seco. Se demuestra que la inversión de flotabilidad tiene lugar para cualquier altura en la que hay mezcla. También se demuestra que la diferenca de temperatura potencial virtual entre la masa de aire mezclada y el aire circundante tiene un valor negativo máximo en la cima de la nube. Se discute el papel de la estructura media en la flotabilidad de las masas de aire mezcladas. Se muestra que la expresión analítica que describe la forma de los diagramas de mezcla es idéntica al criterio de inestabilidad por *entrainment* en la cima de la nube, originalmente obtenido para una capa nubosa de estratocúmulos limitada por una inversión.
Palabras clave: nubes cúmulo, diagramas de mezcla, mezcla lateral, inversión de flotabilidad.

1. INTRODUCTION

Because of the typical positive buoyancies in cumulus clouds the in-cloud vertical velocities tend to be dominated by upward motions. However, various observations and results from large-eddy simulations have shown the presence of cloud downdrafts (Blyth 1993; De Roode and Bretherton 2003). If cloud air is mixed with unsaturated air, evaporation of cloud liquid water will lead to some cooling, which may cause the formation of negatively buoyant cloud downdrafts (Paluch 1979; Raga et al. 1990; Taylor and Baker 1991; Rodts et al 2003).

In this paper mixing diagrams for shallow cumulus are analysed theoretically. It is assumed that cumulus cloud parcels have risen adiabatically to some arbitrary height, where they mix with their surrounding environment. The following two questions will be addressed:

1. What are the minimum buoyancies mixed parcels can obtain?

2. What are the mean thermodynamic conditions necessary for the formation of negatively buoyant mixed cloud parcels?

2. THEORY

In the atmospheric sciences there is a rich variety in the notation for thermodynamic quantities (Bohren and Albrecht 1998). In this paper we will use two conserved variables, i.e. variables that are invariant regarding phase changes, namely the approximated form of the liquid water potential temperature $\theta_l = \theta - L_v/c_p q_l$ and the total specific humidity $q_t = q_v + q_l$, q_v (q_l) the (liquid water) specific humidity, θ the potential temperature, L_v the latent heat of vaporization, c_p the isobaric specific heat for dry air, and $\varepsilon_1 = 1/\varepsilon - 1 \approx 0.608$, where $\varepsilon = R_d/R_v$ the ratio of the specific gas constants for dry air and water vapor. Note that in the absence of cloud liquid water, $\theta_l = \theta$. We neglect the effect of precipitation because both θ_l and q_t are not conserved if liquid water is removed by drizzle.

The virtual potential temperature θ_v can be expressed in terms of conserved variables as,

$$\theta_v = \theta\,(1 + \varepsilon_1 q_t - q_l) = \left(\theta_l + \frac{L_v}{c_p} q_l\right)\left(1 + \varepsilon_1 q_t - \frac{q_l}{\varepsilon}\right) \tag{1}$$

If latent heat is released by condensation of cloud liquid water in an adiabatically rising parcel, θ_v increases with height according to the moist-adiabat $\Gamma_{\theta_{v,moist\_ad}} \equiv (\partial\theta_v/\partial z)_{moist\_ad}$.

Note that if the cloud area fraction is denoted by σ, the horizontal mean value of an arbitrary quantity $\bar{\psi}$ is given by $\bar{\psi} = \sigma\psi_c + (1 - \sigma)\,\psi_e$, where the subscripts *'c'* and *'e'* denote mean in-cloud and environmental values, respectively. For $\sigma << 1$ we can approximate $\psi_e = \bar{\psi}$.

A. DESCRIPTION OF THE MEAN STATE

Figure 1 shows a schematic of a mixed layer capped by a conditionally unstable atmosphere. Cumulus clouds develop from rising plumes that become saturated near the top of the mixed layer. In this study clouds are assumed to rise moist-adiabatically, such that $\theta_{l,c}(z) = \theta_{l,cb}$ and $q_{t,c}(z) = q_{t,cb}$, with the subscript *'cb'* denoting the value of

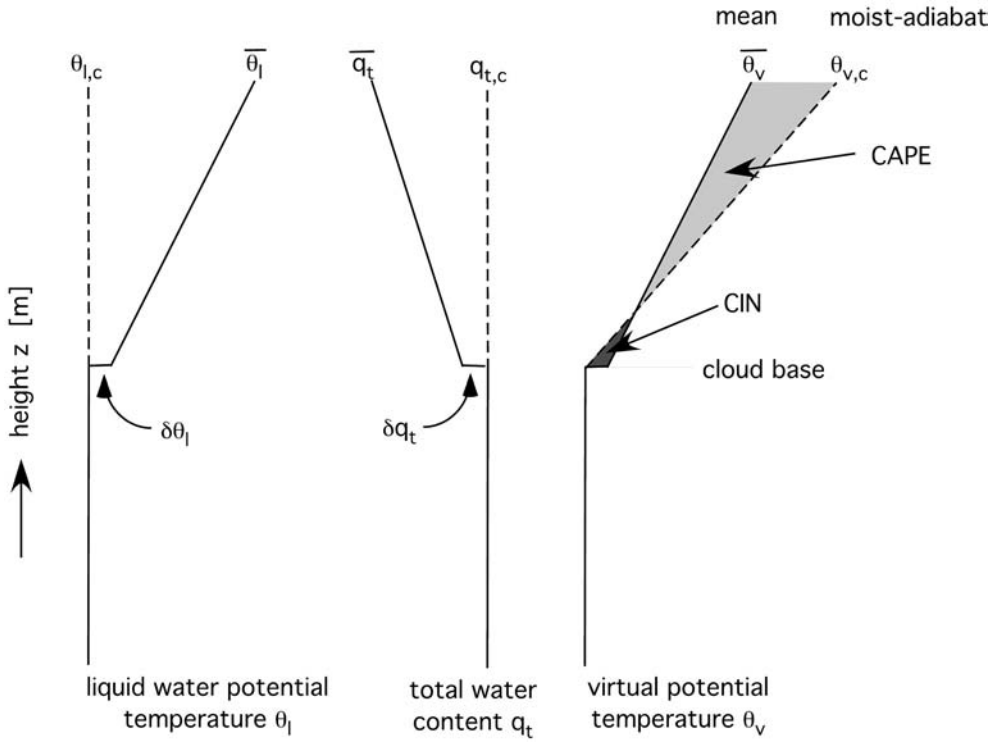

Figure 1.- Schematic of liquid water potential temperature θ_l, total water content q_t and virtual potential temperature θ_v mean vertical profiles in a cumulus cloud layer. Shown are the vertical gradients for an adiabatically rising air parcel that originates in the mixed layer (dashed lines), and the mean state is indicated by solid lines. The grey area indicates CAPE, and the dark shaded area CIN.

a quantity at cloud-base height. Above the mixed layer it is assumed that the mean of $\psi \in \{\theta_l, q_t\}$ can be well described by a linear profile,

$$\overline{\psi}(z') = \psi_c + \delta_\psi + \Gamma_\psi z', \qquad z' = z - z_{cb} > 0 \tag{3}$$

with $\delta_\psi = \overline{\psi}|_{z'=0} - \psi_c$ the difference of ψ between the cloud and its environment at cloud base height, $\Gamma_\psi = \partial\overline{\psi}/\partial z$ represents the mean vertical gradient, and z' the height above cloud base.

To allow the active growth of cumulus clouds the mean virtual potential temperature vertical gradient Γ_{θ_v} must be less than the moist-adiabatic value $\Gamma_{\theta_{v,moist\_ad}}$,

$$\Gamma_{\theta_v} < \Gamma_{\theta_{v,moist\_ad}} \quad \Leftrightarrow \quad \textit{Conditional instability.} \tag{4}$$

Only if this criterion is satisfied, saturated plumes may reach the level of free convection (LFC), above which the plume is positively buoyant. By contrast, in the 'forced cloud' scenario the negative buoyancy below the LFC is sufficient to terminate the upward velocity of the plume, leaving very thin patches of decaying cloudy plumes. This scenario becomes more likely for a larger convective inhibition (CIN), or a smaller vertical plume velocity.

The Δ operator gives the difference of an arbitrary quantity ψ between the cloud's dry environment and the cloud at an arbitrary height z, $\Delta\psi = \psi_e - \psi_c$. In this notation the θ_v difference is given by

$$\Delta\theta_v = \theta_{v,e} - \theta_{v,c} \tag{5}$$

Note that above the LFC the cloud parcel is positively buoyant such that $\Delta\theta_v < 0$.

B. MIXING DIAGRAM

The mixing fraction χ defines the ratio of the environmental air m_2 to the total air mass $m_1 + m_2$,

$$\chi = m_2 / (m_1 + m_2) \tag{6}$$

Suppose an undiluted cloud parcel with properties $q_{t,c}$ and $\theta_{l,c}$ mixes with air from the clear environment at an arbitrary height z_{mix}. At this level the air from the environment has thermodynamic properties and $q_{t,e}|_{z=z_{mix}}$ and $\theta_{l,e}|_{z=z_{mix}}$. In the remainder of the paper ψ_e, ψ_c, and ψ_m refer to the values of ψ at the mixing height z_{mix} in the environment, cloud and the mixed parcel, respectively.

The virtual potential temperature of a mixed parcel $\theta_{v,m}$ as a function of the mixing fraction χ is shown in Figure 2. For a saturated mixed parcel $\chi \leq \chi_*$ the virtual potential temperature as a function of the mixing fraction is given by (Randall 1980; Deardorff 1980; Bretherton et al. 2004),

$$\theta_{v,m} - \theta_{v,c} = \chi\Delta\theta_{v,sat}, \qquad \chi \leq \chi_* \tag{7}$$

where

$$\Delta\theta_{v,sat} \equiv A_w\Delta\theta_l + B_w\Delta q_t = \theta_{v,e} - \theta_{v,sat}|_{z=z_{sat}}, \tag{8}$$

and A_w and B_w are weak functions of the state of the atmosphere (Randall 1980; Deardorff 1980) that incorporate the effect of latent heat release due to evaporation or condensation of cloud liquid water

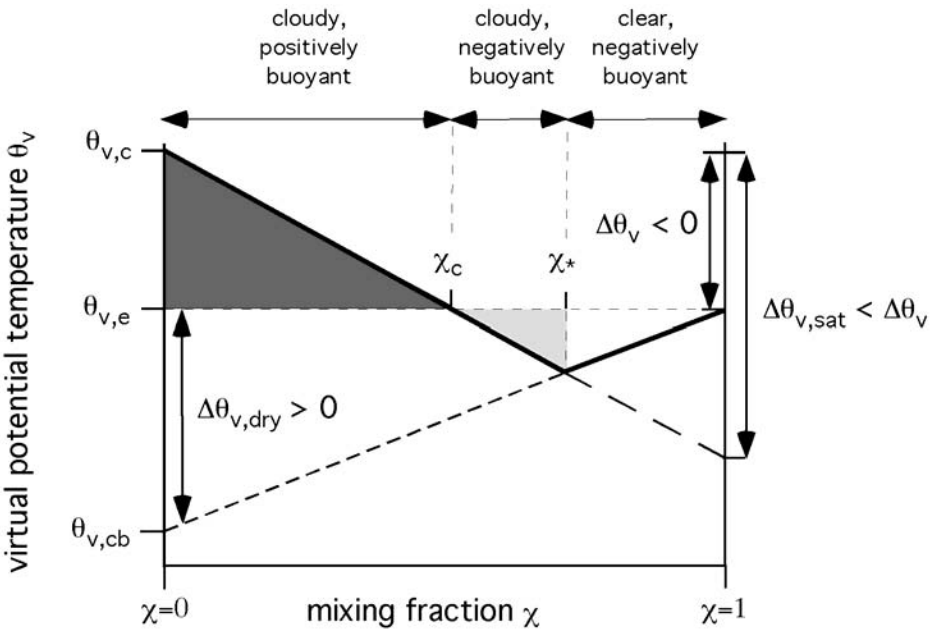

Figure 2.- Schematic of a mixing diagram for an undiluted cumulus cloud parcel that mixes with its dry environment. The solid line shows the virtual potential temperature of a mixed parcel as a function of the mixing fraction. The short and long dashed line denote the dry and saturated mixing lines, respectively. The sign of the jumps follow from the definition of the jumps $\Delta\psi = \psi_e - \psi_c$ and are shown for convenience. See text for more details.

$$A_w = \frac{1 - q_t + \left(q_s + T_0 \dfrac{dq_s}{dT}\right) / \varepsilon}{1 + \dfrac{L_v}{c_p}\dfrac{dq_s}{dT}}, \quad \text{and} \quad B_w = \frac{L_v}{c_p} A_w - T_0, \tag{9}$$

with T_0 a reference temperature and q_s the saturation specific humidity. It is stressed again that $\theta_{v,e}$ in Eq. (8) refers to the virtual potential temperature of the environment at height z_{mix}. For an unsaturated mixed parcel

$$\theta_{v,m} - \theta_{v,e} = (\chi - 1)\Delta\theta_{v,dry}, \qquad \chi_* \le \chi \le 1 \tag{10}$$

with

$$\Delta\theta_{v,dry} \equiv A_d \Delta\theta_l + B_d \Delta q_t = \theta_{v,e} - \theta_{v,cb}, \tag{11}$$

where, to a good approximation, $A_d = 1 + \varepsilon_1 q_{tc}$, $B_d = \varepsilon_1 \theta_{1,c}$ and $\theta_{v,cb} \equiv \theta_{v,c}|_{z=z_{cb}}$.

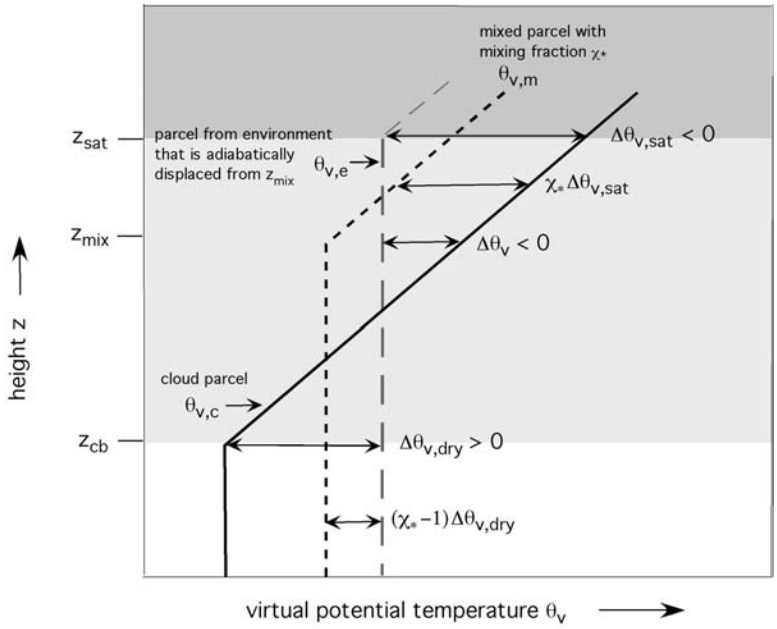

Figure 3.- Schematic showing virtual potential temperature vertical profiles for an adiabatically rising cloud parcel (solid line), for an air parcel from the dry environment that is vertically displaced from its original position at height z_{mix} (long dashed line), and for a mixed parcel with mixing fraction χ_* (short dashed line). The θ_v vertical gradients are either dry- or moist-adiabatic. Below cloud-base height the cloud parcel is unsaturated (unshaded area), and the θ_v difference between the cloud parcel and the displaced dry parcel remains constant at a value $\Delta\theta_{v,dry}$. The parcel from the environment is saturated above its lifting cloud condensation level, $z \geq z_{sat}$ (dark grey shaded area), and the θ_v difference between the cloud and the parcel from the environment remains approximately constant at a value denoted by $\Delta\theta_{v,sat}$. The sign of the jumps follow from the definition of the jumps $\Delta\psi = \psi_e - \psi_c$ and are shown for convenience.

Eqs. (7) and (10) form the basis of our analysis, which will be elaborated in the next section. First we will give an explanation and physical interpretation of the dry and saturated virtual potential temperature jumps.

i. Interpretation of the dry and saturated virtual potential temperature jumps. Why are the dry and saturated jumps involved in the mixing diagram and what is their physical interpretation? To answer these questions, let us perform a thought experiment, as is illustrated schematically in Fig. 3. Assume a mixed parcel which results from mixing air of the cloud and its environment at height z_{mix}. The mixed parcel has a mixing fraction χ_* at which it is just unsaturated and has a virtual potential temperature $\theta_{v,m}$. The latter value will be conserved for downward dry-adiabatic displacement. Likewise, an air parcel from the environment will also maintain its value $\theta_{v,e}$ after an arbitrary vertical displacement but, by contrast, the cloud parcel will obtain a lower value $\theta_{v,cb}$ as it follows the moist-adiabatic lapse rate down to the cloud-base. Recalling that θ_l and q_t will be constant for adiabatic displacement, it appears that for an unsaturated *mixture* it is not relevant whether its

parent parcels are mixed at a height where one of them is saturated, or at a lower height where both are unsaturated. The interpretation is that the condensational heat that a cloud parcel obtains during adiabatic ascent is exactly lost if mixing results in an unsaturated air parcel, such that the 'effective' θ_v of the cloud parcel that goes into the mixture is simply its unsaturated cloud-base value. Therefore, for any unsaturated mixed parcel $(\chi \geq \chi_*)$ its virtual potential temperature can be computed from the dry jump formula (10).

To explain the meaning of the saturated jump $\Delta\theta_{v,sat}$ we now lift both parcels to a level z_{sat} where the dry parcel from the environment becomes just saturated (where we implicitly assume that the dry parcel contains moisture $q_{t,e} > 0$ to allow saturation). Because at z_{sat} both parcels are saturated, the virtual potential temperature of the mixture depends linearly on the mixing fraction χ according to Eq. (7). If the mixed parcel descends back to z_{mix} while being saturated, the θ_v difference with the cloud parcel remains constant along this route as both parcels follow the moist-adiabat. Hence, Eq. (7) is applicable to mixed, saturated parcels, with an interpretation of the saturated jump according to Eq. (8).

3. BUOYANCY REVERSAL

We will explore for which atmospheric conditions negatively buoyant, cloudy mixed parcels can be generated. According to the mixing diagram depicted in Fig. 2 buoyancy reversal occurs for cloudy mixed parcels with mixing fractions $\chi_c < \chi < \chi_*$. The critical mixing fraction χ_c defines a neutrally buoyant mixed parcel, $\theta_{v,m} = \theta_{v,e}$, and can be solved with aid of Eqs. (5) and (7),

$$\chi_c = \frac{\Delta\theta_v}{\Delta\theta_{v,sat}} \,. \tag{12}$$

As can be seen from Fig. 3, and noting that $\Delta\theta_v$ and $\Delta\theta_{v,sat}$ are negative for a conditionally unstable atmosphere, $\Delta\theta_v > \Delta\theta_{v,sat}$, such that $\chi_c < 1$. The critical saturation mixing fraction χ_* corresponds to a just unsatured mixed parcel. At $\chi = \chi_*$, the dry and saturated mixing lines cross. Using Eqs. (7) and (10) gives

$$\chi_* = \frac{\theta_{v,c} - \theta_{v,cb}}{\Delta\theta_{v,dry} - \Delta\theta_{v,sat}} \,. \tag{13}$$

From this equation it follows that

$$\chi_* < 1 \qquad \Leftrightarrow \qquad \Delta\theta_{v,sat} < \Delta\theta_v \,, \tag{14}$$

where we used $\theta_{v,c} - \theta_{v,cb} = \Delta\theta_{v,dry} - \Delta\theta_v$ according to Eq. (11). From Figure 3 it can be seen that this condition is satisfied for a conditionally unstable mean state. We

can further refine the criterion (14) if we realize that cumulus clouds can develop only if the atmosphere is conditionally unstable. In that case above the LFC a moist-adiabatic cloud parcel is positively buoyant with respect to the environment, and $\Delta\theta_v < 0$ according to its definition (5). Hence, for a conditionally unstable atmosphere, $\chi_* < 1$ if $\Delta\theta_{v,sat} < \Delta\theta_v < 0$.

The mixing fractions χ_c and χ_* are related by

$$\chi_c = \frac{\Delta\theta_{v,dry}}{\Delta\theta_{v,sat}} (1 - \chi_*) + \chi_* . \tag{15}$$

If $\chi_* < 1$ it then follows that $\chi_c < \chi_*$. Here we have arrived at an important conclusion, namely that for a conditionally unstable atmosphere mixing fractions $\chi_c < \chi < \chi_*$ exist for which mixed parcels will be cloudy and negatively buoyant with respect to the environment.

A. MEAN STATE STRUCTURE AND MIXING FRACTIONS

To explore the role of the mean state on χ_c and χ_*, we substitute the expression (3) for the mean liquid water potential temperature and the total specific humidity into Eqs. (8) and (11) to give,

$$\Delta\theta_{v,dry} = A_d \left(\Gamma_{\theta_l} z' + \delta_{\theta_l}\right) + B_d \left(\Gamma_{q_t} z' + \delta_{q_t}\right), \tag{16}$$

$$\Delta\theta_{v,sat} = A_w \left(\Gamma_{\theta_l} z' + \delta_{\theta_l}\right) + B_w \left(\Gamma_{q_t} z' + \delta_{q_t}\right), \tag{17}$$

Moreover, for an adiabatic cloud parcel we can write

$$\theta_{v,c}(z') - \theta_{v,cb} = \Gamma_{\theta_{v,moist\_ad}} z'. \tag{18}$$

Eqs. (16)-(18) can be substituted into (12) and (13) to find general solutions for χ_c and χ_*. In case $\delta_\psi << \Gamma_\psi z'$, which applies, for example, well above the cloud base, it turns out that χ_c and χ_* become independent of height,

$$\chi_*(z') = \frac{\Gamma_{\theta_{v,moist\_ad}}}{(A_d - A_w)\,\Gamma_{\theta_l} + (B_d - B_w)\,\Gamma_{q_t}}, \tag{19}$$

$$\chi_c(z') = \frac{\Gamma_{\theta_{v,moist\_ad}} - \left(A_d\Gamma_{\theta_l} + B_d\Gamma_{q_t}\right)}{A_w\Gamma_{\theta_l} + B_w\Gamma_{q_t}}, \tag{20}$$

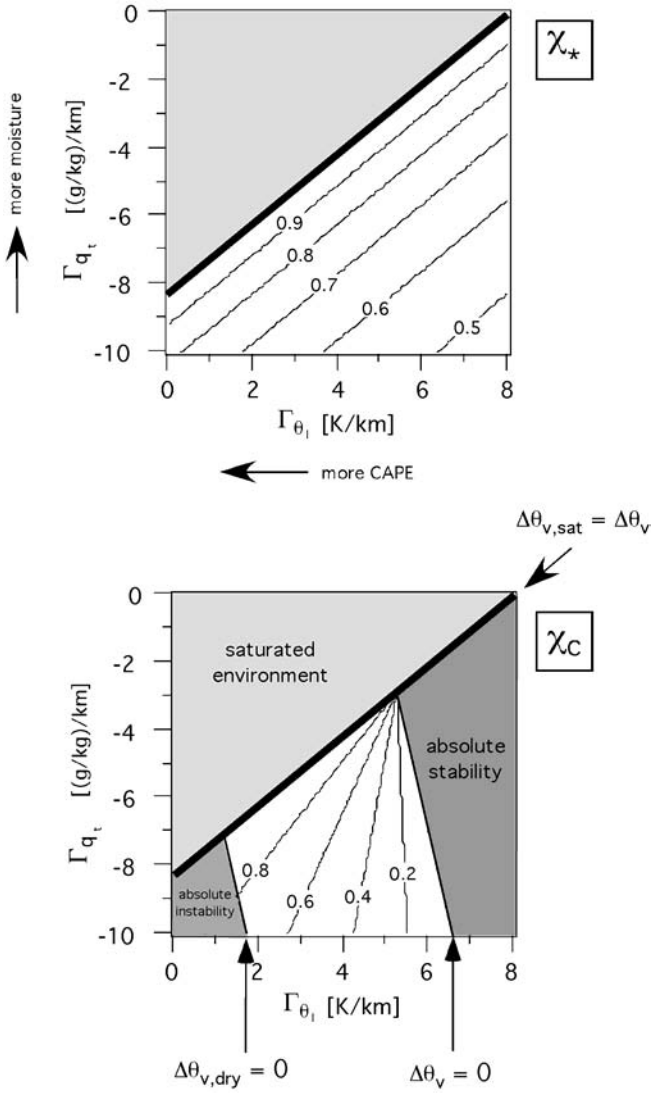

Figure 4.- Contourplots for a) χ_* (upper panel) and b) χ_c (lower panel) computed from Eqs. (19) and (20), respectively, as a function of the mean vertical gradients of the total specific humidity Γ_{q_t} and the liquid water potential temperature Γ_{θ_l}. Because in this example the cloud thermodynamic properties at cloud-base height were taken identical to the mean state at cloud-base height (δ_{θ_l} and δ_{q_t} were taken equal to zero), according to (21) the results apply to any height in the cloud layer. The grey-shaded area indicates a saturated (cloudy) mean state. The arrows in the upper panel indicate the directions into which either CAPE or the mean specific humidity increases. The arrows in the lower plot indicate isolines for which the atmosphere is just absolutely unstable $\Delta\theta_{v,dry} = 0$, just saturated $\Delta\theta_v = \Delta\theta_{v,sat}$, or absolutely stable $\Delta\theta_v = 0$. The numbers used for this example were taken from the BOMEX intercomparison study (Siebesma et al. 2003), with the pressure at cloud base height $p_{cb} = 960\ hPa$, $\theta_{l,c} = 299\ K$, and $q_{t,c} = 17.7\ g\ kg^{-1}$. The cloud layer for the BOMEX case is initialized with vertical gradients $\Gamma_{\theta_l} = 3.85\ K\ km^{-1}$ and $\Gamma_{q_t} = -5.83\ g\ kg^{-1} km^{-1}$.

Figure 4 shows isolines for χ_* and χ_c that are valid over the entire cloud layer as we used $\delta_{\theta_l} = \delta_{q_t} = 0$. Figure 4b distinguishes the following three critical atmospheric states, which boundaries are marked by special solutions for χ_c and χ_*:

I. Absolute stability	$\Delta\theta_v = 0$	$\Leftrightarrow$	$\chi_c = 0.$
II. A just unsaturated mean state	$\Delta\theta_v = \Delta\theta_{v,sat}$	$\Leftrightarrow$	$\chi_* = 1.$
III. Absolute instability	$\Delta\theta_{v,dry} = 0$	$\Leftrightarrow$	$\chi_* = \chi_c.$

In I, the condition $\Delta\theta_v = 0$ implies that the mean vertical gradient of the virtual potential temperature equals the moist-adiabat. For $\Delta\theta_v > 0$, CAPE is negative, and any mixed parcel will be negatively buoyant.

The isoline $\chi_* = 1$ marks the boundary of regime II at which the mean state is just unsaturated. In the interior of regime II the mean state is saturated and cloudy. If $\chi_* = 1$ this means that any lateral mixing will result in saturated mixed air parcels. For values of χ_* close to unity, the moistening due to the cumulus convection may possibly cause a gradual evolution to a stratocumulus-topped boundary layer.

The interpretation of the absolutely unstable regime III is that for very large negative specific humidity gradients the mean virtual potential temperature will decrease with height.

All isolines for χ_c converge to the point $\Delta\theta_v = \Delta\theta_{v,sat} = 0$. Because this condition is a mutual point for regimes I and II, its interpretation is that the mean vertical gradient of the virtual potential temperature follows the moist-adiabat $\Gamma_{\theta_v} = \Gamma_{\theta_{v,moist\_ad}}$ and secondly, that the mean is just unsaturated, $q_{t,e} = q_{sat,e}$. We denote this point as $\Gamma_{\theta_l} = \Gamma_{\theta_*}$.

B. MINIMUM VIRTUAL POTENTIAL TEMPERATURE OF MIXED PARCELS

From the mixing diagram in Figure 2 it can be seen that a mixed parcel obtains a minimum virtual potential temperature $\theta_{v,m,min}$ for a mixing fraction χ_*, so $\theta_{v,m,min} = \theta_{v,m}|_{\chi=\chi_*}$. With aid of Eqs. (10) and (11) the minimum mixed parcel's θ_v with respect to the mean state can be expressed as

$$\delta\theta_{v,m,min} \equiv \theta_{v,m,min} - \theta_{v,e} = (\chi_* - 1)\,\Delta\theta_{v,dry} < 0. \tag{21}$$

The height dependency of $\delta\theta_{v,m,min}$ becomes clear after substitution of Eq. (16) in (21),

$$\delta\theta_{v,m,min} = (\chi_* - 1)\left[A_d\left(\Gamma_{\theta_l} z' + \delta_{\theta_l}\right) + B_d\left(\Gamma_{q_t} z' + \delta_{q_t}\right)\right], \tag{22}$$

Thus $\delta\theta_{v,m,min}$ has its largest negative value at cloud top.

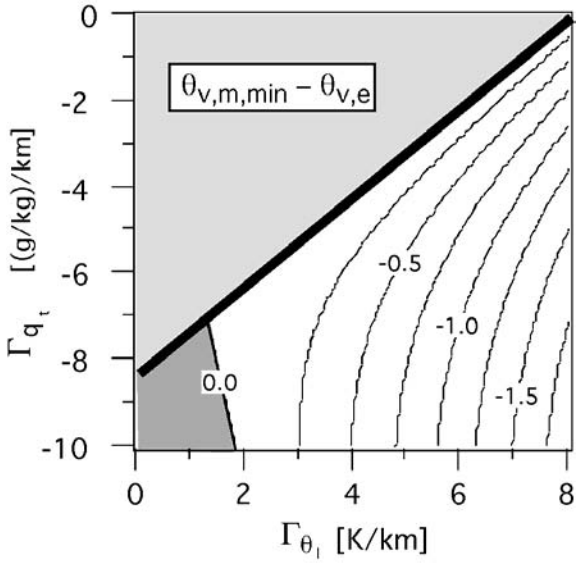

Figure 5.- Same as Figure 4, but for the minimum virtual potential temperature of a mixed parcel relative to the environment, $\delta\theta_{v,m,min} \equiv \theta_{v,m,min} - \theta_{v,e}$ according to Eq. (22). The results were computed for a pressure level at 900 hPa, which corresponds to an approximate height of 560 m above cloud base. The jumps at cloud-base height δ_{θ_l} and δ_{q_t} were set to zero. Note the the x-axis and y-axis can also be interpreted as jumps between the cloud and the environment, as $\Delta\theta_l = \Gamma_{\theta_l} z'$, with $z' = 560$ m, and likewise for the total specific humidity jump.

Figure 5 shows a contour plot of $\delta\theta_{v,m,min}$ computed from Eq. (22). The largest θ_v differences are found for small CAPE and low specific humidities. Also note that the absolute instability regime is marked by isolines of $\delta\theta_{v,m,min} = 0$.

C. BUOYANCY SORTING PARAMETERIZATION SCHEMES

In buoyancy sorting parameterization schemes mixing diagrams are applied to compute lateral mixing rates in cumulus (Kain and Fritsch 1990; Kain 2004; Bretherton et al. 2004). In particular, the buoyancy sorting mechanism applied by Kain and Fritsch (1990) detrains all negatively buoyant mixed air parcels from the cloud updraft. In this way the detrainment rate will depend on χ_c.

Kain (2004) discusses that in buoyancy sorting parameterization schemes entrainment of environmental air is favored when updrafts are much warmer than their environment and/or the environment is relatively moist. He argues that negatively buoyant mixtures are less likely because positive buoyancy is large before mixing and because evaporative cooling potential is limited by the moist environment. From Fig. 4 we find a similar interpretation. CAPE increases if the (liquid water) potential temperature vertical gradient Γ_{θ_l} becomes smaller, which corresponds to increasingly larger values for χ_c. A

similar tendency for χ_c is found if the relative humidity in the cloud layer increases (smaller negative Γ_{q_t}), with a notable exception for conditions where $\Gamma_{\theta_l} > \Gamma_{\theta_*}$.

D. BUOYANCY REVERSAL IN STRATOCUMULUS

With aid of the conserved variables θ_l and q_t we can write

$$\theta_{v,c} - \theta_{v,cb} = \left(A_d \frac{L_v}{c_p} - \frac{\theta_{l,c}}{\varepsilon} \right) q_l \equiv C_l q_l \tag{23}$$

by which we have defined C_l. Furthermore, we used $q_l/\varepsilon << A_d$. Note that the adiabatic liquid water content can be expressed in terms of its moist-adiabatic vertical gradient $\Gamma_{q_{l,moist\_ad}}$,

$$q_l(z') = \Gamma_{q_{l,moist\_ad}} z'. \tag{24}$$

After substitution of Eq. (24) in (23) and using (18), it follows that $C_l = \Gamma_{\theta_{v,moist\_ad}}/\Gamma_{q_{l,moist\_ad}}$. Substitution of Eq. (23) in (13) yields,

$$\chi_* = \frac{C_l q_l}{\Delta\theta_{v,dry} - \Delta\theta_{v,sat}}. \tag{25}$$

Stevens (2002) presents an identical equation to Eq. (25) for a mixture of air from the top of a stratocumulus cloud and air from just above the inversion.

For stratocumulus clouds, one usually defines the inversion jump $\Delta\psi$ by the difference between the values of ψ just above the inversion and near the top of the cloud. Randall (1980) and Deardorff (1980) hypothesized that if the inversion stratification above the stratocumulus cloud top satisfies $\Delta\theta_{v,sat} < 0$, buoyancy reversal could trigger a rapid dissipation of the cloud layer by a positive feedback between the formation of negatively buoyant parcels by entrainment and the subsequent generation of turbulent kinetic energy promoting further entrainment of relatively dry and warm air from just above the inversion. However, because a just unsaturated negatively buoyant air parcel will maintain a constant virtual potential temperature (according to a dry-adiabatic lapse rate) during its descent through the cloud layer, it will rapidly become positively buoyant with respect to the cloud environment as the virtual potential temperature in the cloud layer approximately obeys a moist-adiabatic lapse rate (Roode and Wang 2006). Note that $\Delta\theta_{v,sat}$ can have any sign in stratocumulus-topped boundary layers.

4. SUMMARY AND CONCLUSIONS

It has been demonstrated that mixing air from an adiabatic cumulus cloud with its environment will always result in some mixtures that are cloudy and negatively buoyant. This result can be simply understood by considering an unsaturated mixed parcel. If the mixed parcel does not contain liquid water, the increase in the virtual potential temperature of the cloud parcel by latent heat release during its moist-adiabatic ascent has exactly vanished. This means that the cloud parcel has an 'effective' virtual potential temperature that equals its unsaturated cloud-base value. Consequently, the virtual potential temperature of the unsaturated mixed parcel will then be in between the virtual potential temperature of the mean state at the mixing height and the value of the cloud parcel at the cloud base. Clearly, this results in a mixture that has a lower virtual potential temperature than the mean state value. Note that in the analysis precipitation has been neglected. If drizzle removes a sufficient amount of liquid water, it becomes possible for all mixtures to remain positively buoyant.

It is shown that the minimum buoyancy of a mixed parcel is most negative near cloud top. This finding suggests that the strongest downdrafts will be expected to originate near cloud top, in accord with observations reported by Paluch (1979) and Jonas (1990). The minimum value is dependent on the ambient temperature and humidity. Larger negative buoyancies can be expected for an atmosphere that is relatively dry, and for conditions with just a small amount of CAPE.

Axelsen (2005) used a large-eddy simulation (LES) model to study the role of the mean humidity structure in the cloud layer on the dynamical structure of shallow cumulus clouds. For lower values of the mean specific humidities in the cloud layer the cumuli were found to be less dynamically active due to reduced buoyancies and vice versa. These LES results are in line with the theoretical analysis presented here and in a qualitative agreement with a similar sensitivity study of deep convection performed by Derbyshire et al (2004).

5. ACKNOWLEDGEMENTS

It is a pleasure to thank my colleagues Herve Grenier, Harm Jonker, Pier Siebesma, Margreet van Zanten, Thijs Heus and Simon Axelsen for stimulating feedback on the manuscript.

REFERENCES

AXELSEN, S. L., 2005. The role of relative humidity on shallow cumulus dynamics; results from a Large Eddy Simulation model. Master thesis. Institute for Marine and Atmospheric research Utrecht (IMAU), Princetonplein 5, 3584 CC, Utrecht, The Netherlands.

BLYTH, A. M., 1993. Entrainment in cumulus clouds. *J. Appl. Meteor.,* 32, 626-641.

BOHREN, C. F. & B. A. ALBRECHT, 1998. *Atmospheric Thermodynamics*, Oxford University Press, 402 pp.

BRETHERTON, C. S., J. R. MCCAA & H. GRENIER, 2004. A new parameterization for shallow cumulus convection and its application to marine subtropical cloud-topped boundary layers. Part I: Description and 1D results, *Mon. Wea. Rev*., 132, 864-882.

DERBYSHIRE, S. H., I. BEAU, P. BECHTOLD, J. Y. GRANDPEIX, J. M. PIRIOU, J. L. REDELSPERGER & P. M. M. SOARES, 2004. Sensitivity of moist convection to environmental humidity. *Quart. J. Roy. Meteor. Soc.,* 128, 1-26.

DE ROODE, S. R. & C. S. BRETHERTON, 2003: Mass-flux budgets of shallow cumulus clouds, *J. Atmos. Sci*., 60, 137-151.

DE ROODE, S. R. & Q. WANG, 2006: Do stratocumulus clouds detrain? FIRE I data revisited, *Bound.-Layer Meteor.*, 122, 479-491.

DEARDORFF, J. W., 1980. Cloud-top entrainment instability, *J. Atmos. Sci*., 37, 131-147.

JONAS, P. R., 1990. Observations of cumulus cloud entrainment, *Atm. Res*., 25, 105-127.

KAIN, J. S., 2004. The Kain-Fritsch convective parameterization: An update, *J. Appl. Meteor.,* 43, 170-181.

KAIN, J. S. & J. M. FRITSCH, 1990. A one-dimensional entraining/detraining plume model and its application in convective parameterization, *J. Atmos. Sci*., 47, 2784-2802.

PALUCH, I. R., 1979. The entrainment mechanism in Colorado cumuli, *J. Atmos. Sci*., 36, 2467-2478.

RAGA, G. B., J. B. JENSEN & M. B. BAKER, 1990. Characteristics of cumulus band clouds off the coast of Hawaii, *J. Atmos. Sci*., 47, 338-355.

RANDALL, D. A., 1980. Conditional instability of the first kind upside down, *J. Atmos. Sci*., 37, 125-130.

RODTS, S. M. A., P. G. DUYNKERKE & H. J. J. JONKER, 2003. Size distributions and dynamical properties of shallow cumulus clouds from aircraft observations and satellite data, *J. Atmos. Sci*., 60, 1895-1912.

SIEBESMA, A. P., C. S. BRETHERTON, A. BROWN, A. CHLOND, J. CUXART, P. G. DUYNKERKE, H. JIANG, M. KHAIROUTDINOV, D. LEWELLEN, C.-H. MOENG, E. SANCHEZ, B. STEVENS & D. E. STEVENS, 2003. A large eddy simulation intercomparison study of shallow cumulus convection, *J. Atmos. Sci*., 60, 1201-1219.

STEVENS, B., 2002. Entrainment in stratocumulus-topped mixed layers, *Quart. J. Roy. Meteor. Soc.,* 128, 2663-2690.

TAYLOR, G. R., & M. B. BAKER, 1991. Entrainment and detrainment in cumulus clouds, *J. Atmos. Sci*., 48, 112-121.